Macroalgae of *Iridaea cordata* as an efficient biosorbent to remove hazardous cationic dyes from aqueous solutions

Leticia Belén Escudero, Patricia Nora Smichowski and Guilherme Luiz Dotto

ABSTRACT

In the present work, *Iridaea cordata* (*IC*), a red marine macroalgae, was used as an efficient biosorbent for the removal of crystal violet (CV) and methylene blue (MB) dyes from aqueous solutions. The effects of pH (5, 7, and 9) and *IC* concentration (1, 3, and 5 g L^{-1}) on the biosorption were studied through a 3^2 full factorial design. Under the optimal conditions (pH: 7, biosorbent concentration: 1 g L^{-1}), biosorption kinetic studies were developed and the obtained experimental data were evaluated by pseudo-first order and pseudo-second order models. The results showed that the pseudo-second order model was in agreement with the experimental kinetic data for both dyes. Equilibrium studies were also carried out, and results exhibited good concordance with the Brunauer–Emmett–Teller isotherm. The biosorption capacities were 36.5 and 45.0 mg g^{-1} for CV and MB dyes, respectively. The dye removal percentages were around 75% for CV and 90% for MB. Thermodynamically, the biosorption process proved to be exothermic, spontaneous, and favorable. These results showed that *IC* biomass is a promising biosorbent for removal of CV and MB dyes from aqueous solutions.

Key words | algae, biosorption, cationic dyes, kinetic, thermodynamic

Leticia Belén Escudero (corresponding author)
Laboratory of Analytical Chemistry for Research and Development (QUIANID), Facultad de Ciencias Exactas y Naturales,
Universidad Nacional de Cuyo,
Padre J. Contreras 1300, Mendoza 5500,
Argentina
E-mail: *letibelescudero@gmail.com*

Leticia Belén Escudero
Patricia Nora Smichowski
Consejo Nacional de Investigaciones Científicas y Técnicas (CONICET), Buenos Aires,
Argentina

Patricia Nora Smichowski
Comisión Nacional de Energía Atómica, Gerencia Química,
Av. General Paz 1499, Buenos Aires B1650KNA,
Argentina

Guilherme Luiz Dotto
Chemical Engineering Department,
Federal University of Santa Maria–UFSM,
1000 Roraima Avenue, Santa Maria, RS,
Brazil

INTRODUCTION

Crystal violet (CV) and methylene blue (MB) dyes are contaminants that are introduced into the environment mainly as waste from textile industries. These dye molecules remain in the environment for a long period, causing several disorders for human health, including eyes burn, allergy, cyanosis, and skin irritation (Mittal *et al.* 2010). Their ingestion can cause irritation in the gastrointestinal tract, increase the heart rate, and cause headache, nausea, and mental confusion (Rafatullah *et al.* 2010). Furthermore, these organic compounds are potentially hazardous for the aquatic ecosystems, as they cause inhibition of the photosynthesis, thus generating consequences such as a decrease in the growth speed or even the death of aqueous flora (Yang *et al.* 2015). Therefore, considerable interest in developing more studies devoted to the removal of MB and CV dyes from aqueous media has arisen in the research field.

Operations based on biological treatment (Yahiaoui *et al.* 2013), coagulation and electrocoagulation (Anantha Singh & Ramesh 2013; Mbacké *et al.* 2016), membrane filtration (Cheng *et al.* 2011; Liang *et al.* 2011), oxidation (Jana *et al.* 2010; Ünnü *et al.* 2016), electrochemical oxidation (Zhang *et al.* 2010; Yao *et al.* 2013), and adsorption/biosorption (Sharma *et al.* 2011; Ahmed 2016; Umpierres *et al.* 2017) have been applied for the removal of MB and CV from contaminated wastewaters. Among them, biosorption is one of the most convenient methods to remove contaminants due to being a low-cost, simple, and efficient operation. In the case of adsorption, activated carbon is the most common adsorbent used for dye removal due its outstanding properties, such as good pore structures and high specific surface area. However, the treatment of contaminated water with activated carbon is not always feasible due to its high cost (Moreno-Castilla & Rivera-Utrilla 2001). For this reason, cheaper and effective alternatives need to be explored.

Several works have reported the use of dead macroalgae for the removal of contaminants (Rubín *et al.* 2010; Esmaeili

doi: 10.2166/wst.2017.505

& Darvish 2014; Anastopoulos & Kyzas 2015; Devi & Murugappan 2016; Castro *et al.* 2017; Dadwal & Mishra 2017). This kind of biosorbent shows outstanding properties, including a large area/volume ratio, low cost, and relatively simple growth (Suresh & Ravishankar 2004; Escudero *et al.* 2016). To date, there are no biosorption studies reported in the literature using *Iridaea cordata* (*IC*) biomass for the removal of toxic compounds. This biomass is a cold- and dry-adapted red alga occurring in North and South America, Australia, New Zealand, and Antarctica (Navarro *et al.* 2010; Rautenberger *et al.* 2015). As for all red algae, the cell wall of *IC* is composed of agar, carrageenan, xylans, lectin and cellulose. The wide variety of functional groups present in these molecules could be involved in the biosorption process. Moreover, this alga is abundant and has the ability to maintain its functioning photosynthetic apparatus even in darkness and winter (Weykam *et al.* 1997). *Iridaea cordata* has been defined as an opportunistic life strategist and hence it is easy to cultivate under different laboratory conditions (Weykam *et al.* 1997). For these reasons, the aim of our work is to contribute novel information through the evaluation of the biosorbent potential of *IC* biomass for the removal of hazardous cationic dyes from aqueous solutions. This work opens the door for new studies in this field. The algae can be cultivated under different conditions, which generates biomasses with different functional groups and, hence, the possibility of its use to remove specific contaminants from aqueous media. In this study, the *IC* biosorbent was evaluated for removal of CV and MB dyes. The characteristics of the biosorbent were evaluated by the point of zero charge (pH_{PZC}), Fourier transform infrared (FTIR) spectroscopy, scanning electron microscopy (SEM) and energy X-ray dispersive spectroscopy (EDS). A 3^2 full factorial design was developed to optimize the pH and biosorbent concentration. The biosorption kinetic data were evaluated by the pseudo-first order and pseudo-second order model. The Brunauer–Emmett–Teller (BET) model was used to fit the biosorption equilibrium data. Thermodynamic parameters of standard Gibbs free energy change, standard enthalpy change, and standard entropy change were also estimated.

MATERIALS AND METHODS

Solutions and reagents

CV dye (tris(4-(dimethylamino)phenyl)methylium chloride; C.I. 42555; $\lambda_{max} = 583$ nm; molecular formula $C_{25}H_{30}N_3$; molecular weight 407.99 g mol^{-1}) was obtained from Vetec (Brazil). MB dye (3,7-bis(dimethylamio)-phenothiazin-5-ium chloride; C.I. 52030; $\lambda_{max} = 664$ nm; molecular formula $C_{16}H_{18}N_3SCl$; molecular weight 319.8 g mol^{-1}) was obtained from Merck Ltda (Brazil). Stock standard solutions of 1,000 mg L^{-1} were prepared from an accurate weight of CV and MB dissolved in deionized water. Working standard solutions were prepared by appropriate dilution with deionized water. The pH of the solution was adjusted with 0.1 mol L^{-1} NaOH and HCl solutions using a pH meter (Digimed, DM 20, Brazil) for the measurements.

Preparation of algal adsorbent

The algal biomass was collected at locations in the vicinity of Casey Station in the Windmill Islands, East Antarctica. Macroalgae were transported in polyethylene containers to the laboratory, where they were first washed with drinking water and then rinsed with distilled water several times to remove extraneous and salts. After, the biomass was oven dried at 50 °C for 24 h, and stored in a desiccator. Finally, it was ground in a blender until particles with an average size of 1 mm, a BET surface area of 45 m^2 g^{-1} and pore volume of 0.092 cm^3 g^{-1} were obtained.

Methodologies used for macroalgae characterization

In order to know the surface charge of the biosorbent as a function of pH, pH_{PZC} was determined following a procedure similar to that reported by Rivera-Utrilla *et al.* (2001). Initially, 50 mL of 0.01 mol L^{-1} NaCl solutions was placed in closed Erlenmeyer flasks. The pH values were adjusted to 2, 4, 6, 8, 10, and 12 by the addition of 0.1 mol L^{-1} NaOH or HCl solutions. Then, an amount of 0.15 g of the biosorbent was added and the final pH was determined after 48 h under agitation at room temperature. The pH_{PZC} is the point where the curve of pH_{final} vs. $pH_{initial}$ intersects the line $pH_{initial} = pH_{final}$.

FTIR spectroscopy (Shimadzu, Prestige 21, Japan) was used for the identification of functional groups present in the biosorbent (Silverstein *et al.* 2007). Samples were analyzed using potassium bromide (KBr) pellets (~0.5 mg sample with 100 mg KBr and compressing the mixture into a 13-mm diameter pellet).

The morphology of the biosorbent and the main elements present on the alga surface were evaluated by SEM coupled to EDS (Jeol, JSM-6610LV, Japan). Before analysis, samples were coated with a 15-nm thick Au/Pd layer with a sputter coating system. Both FTIR and SEM

analytical techniques were performed before and after the biosorption process in order to identify possible changes on the biosorbent surface.

Biosorption experiments

The biosorption experiments used to perform the experimental design were carried out as follows. Erlenmeyer flasks containing 25 mL of 50 mg L^{-1} CV or MB solutions were prepared. The pH of each dye solution was adjusted to different pH values (3, 5, and 7). Then, different amounts of the algal biosorbent (25, 50, and 125 mg) were individually added to the previous solutions. The flasks were stirred at 200 rpm in a thermostatic agitator (Marconi, MA 093, Brazil) for 90 min at room temperature. Finally, the solid phase was separated from the supernatant using a centrifuge (Centribio, 80-2B, Brazil) at 3,500 rpm for 10 min.

Subsequently, the kinetic experiments were carried out under the optimal conditions (above determined). Thus, 25 mL of dye solution (CV or MB), with initial dye concentrations of 50 and 100 mg L^{-1} were used. The pH was adjusted to 7. An amount of 25 mg of biosorbent was added to each solution. Contact times from 0 to 120 min were assayed (samples were withdrawn at different time intervals), at room temperature and under stirring rate of 200 rpm.

The equilibrium experiments were assayed in a thermostatic agitator at 298, 308, 318, and 328 K. Erlenmeyer flasks containing 25 mL of CV or MB solution with initial concentrations of 25, 50, 100, 150, 200, and 300 mg L^{-1} were prepared and the pH of each solution was also adjusted to 7. The flasks were placed in the thermostatic agitator to reach the suitable temperature. Then, 25 mg of *IC* biosorbent was added to each flask. The flasks were stirred at 200 rpm until the equilibrium. Finally, the solid phase was separated by centrifugation.

For all experiments, the CV and MB concentrations were determined in the upper aqueous phase by spectrophotometry (Biospectro SP-22, Brazil), at the maximum wavelength for each dye. Calibration was performed against aqueous standards and blank solutions. The dye removal percentage (R, %) was calculated by Equation (1). Biosorption capacity at any time (q_t (mg g^{-1})) and at equilibrium (q_e (mg g^{-1})) were calculated by Equations (2) and (3), respectively (Crini & Badot 2008):

$$R = \frac{(C_0 - C_e)}{C_0} 100 \quad (1)$$

$$q_t = \frac{V(C_0 - C_t)}{m} \quad (2)$$

$$q_e = \frac{V(C_0 - C_e)}{m} \quad (3)$$

where C_0 is the initial dye concentration in liquid phase (mg L^{-1}), C_t is the dye concentration in liquid phase at any time t (mg L^{-1}), C_e is the equilibrium dye concentration in liquid phase (mg L^{-1}), m is the amount of adsorbent (g) and V is the volume of solution (L).

Experimental design and optimization of variables

As pH and biosorbent dosage play an important role in the biosorption process, the effects of pH (5, 7, and 9) and biomass concentration (1, 3, and 5 g L^{-1}) on the biosorption capacity were evaluated through a three-level two-factor 3^2 full factorial design. The biosorption capacity (q) was represented as a function of independent variables, through the polynomial quadratic equation expressed in Equation (4):

$$q = a + \sum_{i=1}^{n} b_i x_i + \sum_{i=1}^{n} b_{ii} x_i^2 + \sum_{i=1}^{n-1} \sum_{j=i+1}^{n} b_{ij} x_i x_j \quad (4)$$

where, a is the constant coefficient, b_i are the linear coefficients, b_{ij} are the interaction coefficients, b_{ii} are the quadratic coefficients, and x_i and x_j are the coded values of the variables. The statistical significance of the nonlinear regression was determined by Student's t-test, the second order model equation was evaluated by Fisher's test and the proportion of variance explained by the model obtained was given by the coefficient of determination, R^2. Experimental runs were performed at random and the results were analyzed using Statistica version 9.1 (StatSoft Inc., USA) software.

Kinetic studies

Kinetic profiles of CV and MB biosorption on *IC* marine algae were developed by fitting the experimental data using the pseudo-first order (Lagergren 1898), and pseudo-second order (Ho & McKay 1998) models. These models are shown in Equations (5) and (6), respectively:

$$q_t = q_1(1 - \exp(-k_1 t)) \quad (5)$$

$$q_t = \frac{t}{(1/k_2 q_2^2) + (t/q_2)} \quad (6)$$

where k_1 and k_2 are the rate constants of pseudo-first order (min^{-1}) and pseudo-second order ($g\,mg^{-1}\,min^{-1}$) models, respectively; q_1 and q_2 are the theoretical values for the biosorption capacity ($mg\,g^{-1}$).

Equilibrium models

The BET model was tested aiming to represent the CV and MB biosorption on *IC* biomass. This model assumes sites with different energies on the surface of the adsorbent; consequently, multilayers can be formed in several parts of this surface. It is represented by Equation (7) (Brunauer *et al.* 1938):

$$q_e = \frac{q_{BET} K_1 C_e}{(1 - K_2 C_e)(1 - K_2 C_e + K_1 C_e)} \tag{7}$$

where q_{BET} is the monolayer biosorption capacity ($mg\,g^{-1}$), K_1 and K_2 are the BET constants ($L\,mg^{-1}$).

Thermodynamic studies

The biosorption of CV and MB on *IC* alga was thermodynamically evaluated according to the standard values of Gibbs free energy change (ΔG^0, $kJ\,mol^{-1}$), enthalpy change (ΔH^0, $kJ\,mol^{-1}$), and entropy change (ΔS^0, $kJ\,mol^{-1}\,K^{-1}$), which were estimated by Equations (8)–(10) (Milonjic 2007; Anastopoulos & Kyzas 2016):

$$\Delta G^0 = -RT \ln(\rho K_e) \tag{8}$$

$$\Delta G^0 = \Delta H^0 - \Delta S^0 T \tag{9}$$

$$\ln(\rho K_e) = \frac{\Delta S^0}{R} - \frac{\Delta H^0}{RT} \tag{10}$$

where K_e is the equilibrium constant ($L\,g^{-1}$) (based on the parameters of the best fit isotherm model), T is the temperature (K), R is 8.31×10^{-3} kJ mol $^{-1}$ K^{-1} and ρ is the solution density ($g\,L^{-1}$).

Modeling and parameter estimation

The kinetic, equilibrium and thermodynamic parameters were determined by nonlinear regression using Statistic 9.1 software (Statsoft, USA). The fit quality was checked through R^2 and average relative error (*ARE*) (Equations (11) and (12)):

$$R^2 = \left(\frac{\sum_i^n \left(q_{i,exp} - \bar{q}_{i,exp}\right)^2 - \sum_i^n \left(q_{i,exp} - q_{i,model}\right)^2}{\sum_i^n \left(q_{i,exp} - \bar{q}_{i,exp}\right)^2} \right) \tag{11}$$

$$ARE = \frac{100}{n} \sum_{i=1}^{n} \left| \frac{q_{i,\mathrm{model}} - q_{i,\mathrm{exp}}}{q_{i,\mathrm{exp}}} \right| \tag{12}$$

where $q_{i,model}$ is each value of q predicted by the fitted model, $q_{i,exp}$ is each value of q measured experimentally, $\bar{q}_{i,\mathrm{exp}}$ is the average of q experimentally measured, and n is the number of experimental points.

RESULTS AND DISCUSSION

IC biomass characteristics

Iridaea cordata biosorbent was characterized according to the pHPZC, FTIR spectroscopy, SEM, and EDS. The pH_{PZC} of the marine algae was 6.80, which means that at pH values lower than 6.80, the surface charge of the biosorbent is positively charged. In contrast, if the pH is higher than 6.80, the surface of the algae is negatively charged.

FTIR spectroscopy was used in order to understand the possible interactions between the functional groups present in the biosorbent surface and the cationic dyes. As can be seen in Figure 1, the FTIR spectrum of *IC* biomass shows a broad band at 3,433 cm^{-1}, which is mainly due to O–H and N–H stretching (Coates 2000). The band visualized at

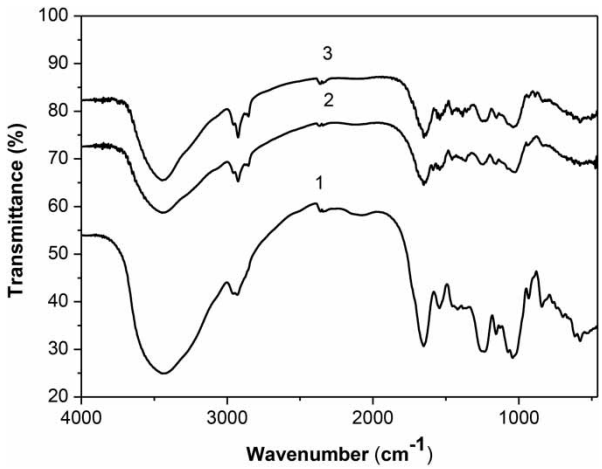

Figure 1 | FTIR spectra of *IC* biomass before (1) and after CV (2) and MB (3) biosorption.

2,930 cm^{-1} is assigned to stretching vibrations of the C–H bond of the aliphatic groups (Coates 2000). The band found at 1,640 cm^{-1} can be attributed to stretching of the conjugated carbonyl bond in the lignin that is present in *IC* biomass (Chen *et al.* 2011; Song *et al.* 2011). The bands at 1,644 and 1,546 cm^{-1} can be attributed to C = O stretching vibration and a combination of N–H bending and C–N stretching vibrations in amide compounds (Duygu *et al.* 2012). The bands at 1,230 to 1,265 cm^{-1} are assigned to the aryl–O stretching of the aromatic ethers (Coates 2000). The bands present at 1,042 and 1,153 cm^{-1} could be attributed to C–O–C stretching of ether (Coates 2000). The bands at 929 and 842 cm^{-1} could represent the j-carrageenans present in *IC* algae (Vijayaraghavan *et al.* 2015). The band at 847 cm^{-1} may correspond to the S = O stretching (Coates 2000). The weak band found at 620 cm^{-1} could be due to C–S and C = S stretching (Kannan 2014). The analysis of the *IC* spectrum reveals that the biosorbent contains several functional groups that could interact with CV and MB dyes. The spectra after biosorption with CV and MB (Figure 1) did not show significant changes with respect to the spectra of raw biomass. It means that no chemical links were formed or broken during the biosorption process, indicating that a physical process occurred.

Figure 2 shows the SEM images of *IC* biosorbent before (Figure 2(a) and 2(b)) and after the biosorption of CV (Figure 2(c)) and MB (Figure 2(d)). It can be observed that *IC* biomass is composed of amorphous particles dispersed on the rough surface (Figure 2(a) and 2(b)). This morphology is suitable to accommodate the molecules of CV and MB on the surface of the biomass. After biosorption of CV (Figure 2(c)) and MB (Figure 2(d)), a change (smoothing) in the surface texture of the biosorbent can be observed, which manifests the biosorption of the colored solutions on the algae surface.

Figure 3 exhibits the EDS spectra of *IC* biosorbent before (Figure 3(a)) and after biosorption process for CV (Figure 3(b)) and MB (Figure 3(c)) dyes. It can be observed that the marine algae contain elements such as C, O, Fe, Na, Mg, Al, Si, P, S, Cl, K, and Ca, which is in concordance with the biological matrix. After biosorption of dyes, some elements

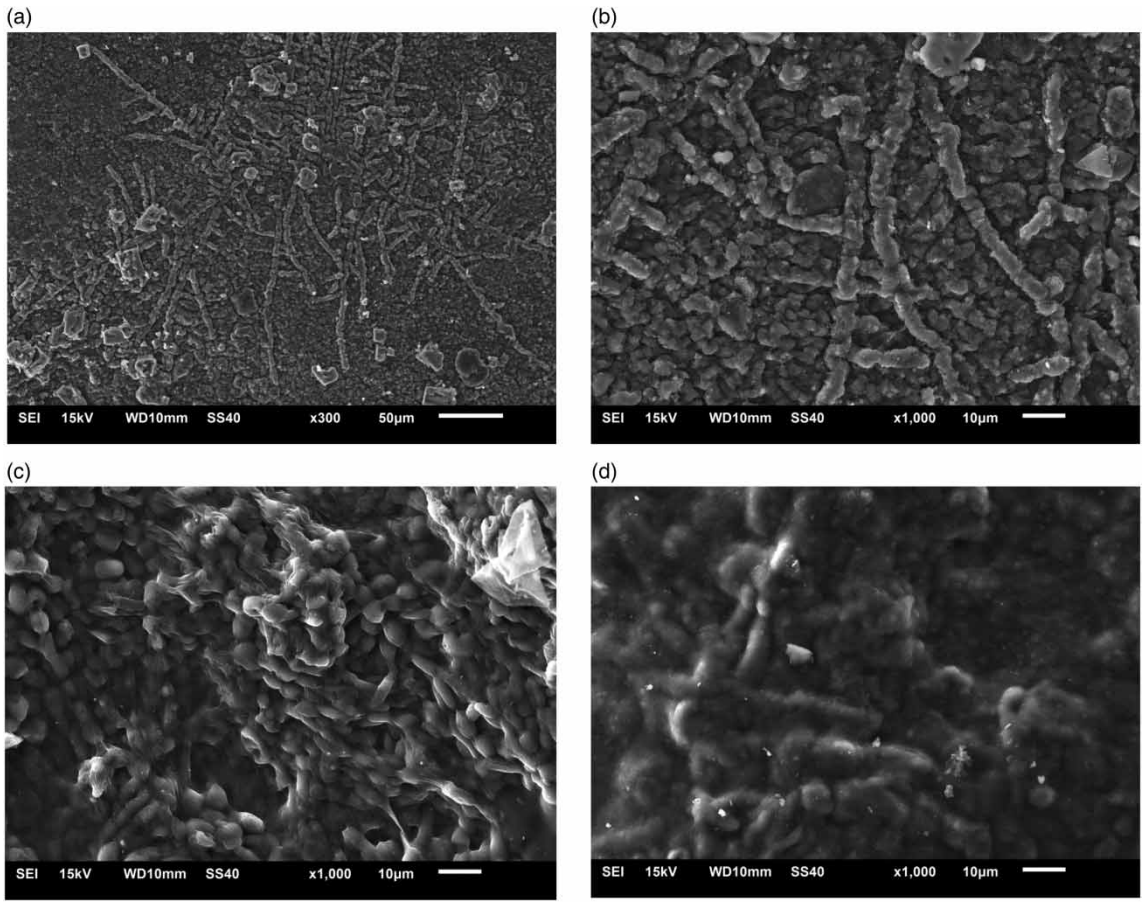

Figure 2 | SEM images of *IC* biomass before (a), (b) and after CV (c) and MB (d) biosorption.

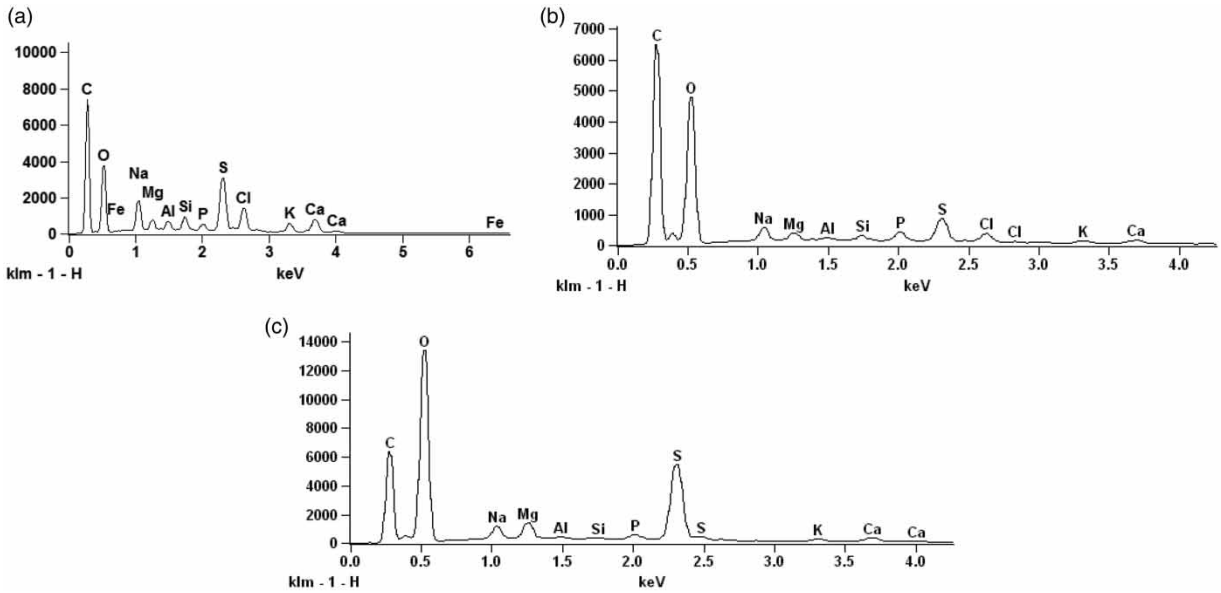

Figure 3 | EDS spectra of *IC* biosorbent before (a) and after the biosorption process for CV (b) and MB (c).

cannot be observed in the spectra. In both cases, Fe is not present after the biosorption process. It could suggest that an ion-exchange could be one of the mechanisms involved in dye removal. In the case of MB biosorption, chloride is also absent, and the percentage of sulfur is higher in comparison with the raw biomass. This suggests the insertion of sulfhydryl groups of the organic molecule on the adsorbent surface.

Optimization of cationic dye biosorption

Table 1 shows the experimental design matrix and the results obtained thought the 3^2 full factorial design.

The significance of pH and biosorbent concentration on the biosorption capacity was evaluated by the Pareto charts, shown in Figure 4.

In the Pareto charts, the independent variables (represented by horizontal bars) are in the y axis and the standardized effects are in the x axis. The significance level ($p = 0.05$) is represented by a vertical dashed line. If the horizontal bars cross the vertical dashed line, then the independent variable significantly affects the response (biosorption capacity for each dye). Furthermore, if the horizontal bars have positive values, then the independent variable affects the response by a directly proportional

Table 1 | Experimental design matrix and results for CV and MB biosorption by *IC* biomass

			CV		MB	
Experiment	**pH [coded form]**	**IC concentration ($g\,L^{-1}$) [coded form]**	***R* (%)[a]**	***q* ($mg\,g^{-1}$)**	***R* (%)[a]**	***q* ($mg\,g^{-1}$)**
1	5 [−1]	1 [−1]	71.2 ± 2.5	34.9 ± 2.8	90.1 ± 3.1	41.1 ± 2.6
2	5 [−1]	3 [0]	72.1 ± 2.9	11.9 ± 1.8	89.4 ± 2.7	14.7 ± 1.5
3	5 [−1]	5 [+1]	75.8 ± 3.4	7.60 ± 2.1	89.5 ± 2.5	8.8 ± 1.4
4	7 [0]	1 [−1]	73.0 ± 3.1	36.5 ± 3.1	90.8 ± 3.0	45.0 ± 2.7
5	7 [0]	3 [0]	73.8 ± 3.1	12.0 ± 1.8	89.8 ± 3.1	14.9 ± 1.4
6	7 [0]	5 [+1]	76.4 ± 2.6	7.60 ± 2.1	89.1 ± 2.8	8.8 ± 1.5
7	9 [+1]	1 [−1]	72.4 ± 3.2	34.3 ± 2.7	90.0 ± 2.7	44.6 ± 2.6
8	9 [+1]	3 [0]	73.9 ± 2.9	12.1 ± 1.9	90.0 ± 3.1	14.4 ± 1.6
9	9 [+1]	5 [+1]	75.5 ± 3.3	7.52 ± 1.7	89.9 ± 3.3	8.9 ± 1.7

R: dye removal percentage; *q*: biosorption capacity.
[a]Mean ± standard deviation (n = 3).

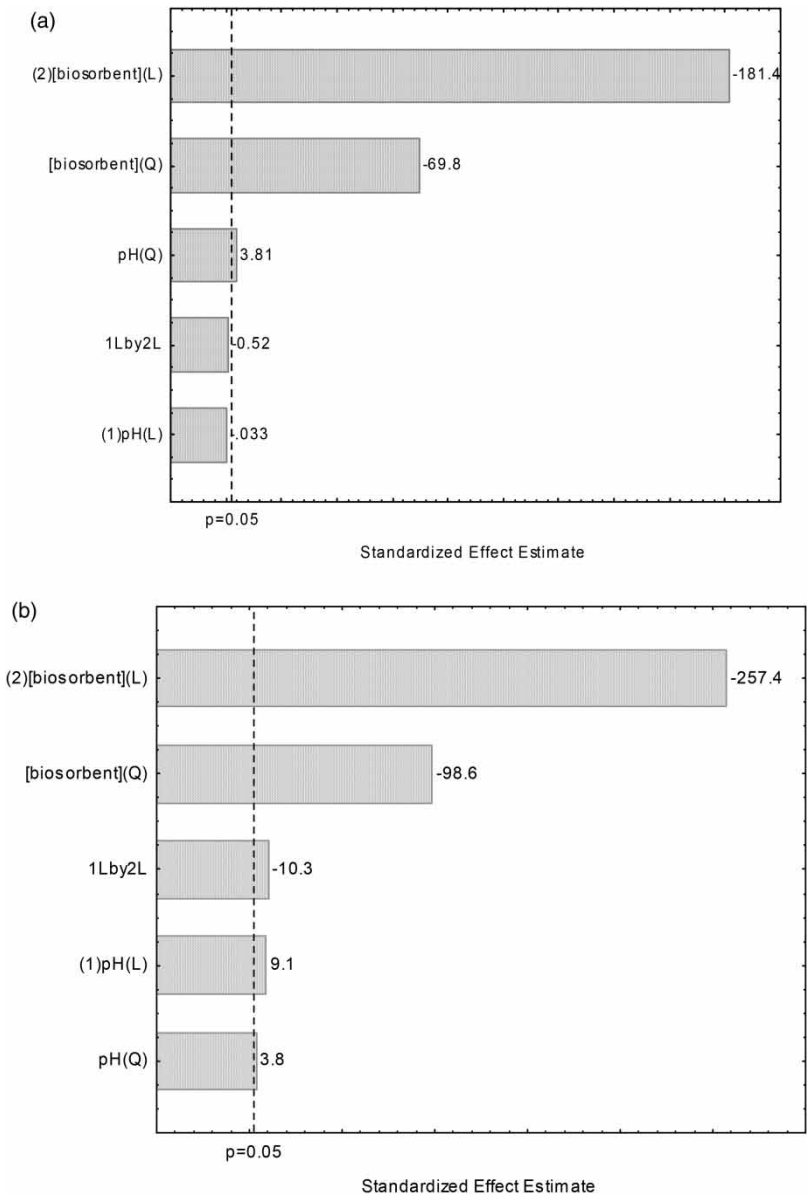

Figure 4 | Pareto charts of cationic dye biosorption capacity of *IC*: (a) CV and (b) MB.

manner. In the same way, if the bars have negative values, the influence is inversely proportional. For the biosorption capacity of CV (Figure 4(a)), it can be seen that linear and quadratic effects belonging to algae concentration were highly significant ($p \leq 0.05$). Regarding pH, only the quadratic effect was slightly significant ($p \leq 0.05$). For the biosorption capacity of MB, all the linear and quadratic effects and the interaction effects were significant ($p \leq 0.05$). However, it is clear that the effect of *IC* concentration was the most significant factor, whereas pH showed minimal effects.

The biosorption capacities of CV and MB as function of *IC* concentration (x_1) and pH (x_2) are depicted in Equations (13) and (14), respectively:

$$q_{CV} = 12.4 + 9.2\,x_1^2 - 0.5\,x_2^2 - 13.8\,x_1 \tag{13}$$

$$q_{MB} = 14.9 + 11.4\,x_1^2 - 0.4\,x_2^2 - 17.2\,x_1 + 0.6\,x_2 - 0.8\,x_1x_2 \tag{14}$$

In order to verify the prediction and significance of the models, analysis of variance and Fisher F-test were used. The

biosorption model for CV proved to be significant and predictive, since calculated Fisher ($F_{calc} = 3{,}740$) was more than 1,000 times greater than the standard Fisher ($F_{std} = 3.34$), with R^2 of 0.99. The model for MB was also significant and predictive, with a calculated Fisher ($F_{calc} = 2{,}561$) 800 times higher than standard Fisher ($F_{std} = 3.1$), with $R^2 = 0.99$.

Response surface methodology is an interesting tool for multivariate optimization because it combines statistical experimental designs that can be used to describe the individual and cumulative effect of the evaluated variables on a response and determines the mutual interactions between the evaluated variables and their subsequent effect on the response. In this work, a representation of biosorption capacities vs. *IC* concentration and pH variables through graphics of response surface is shown in Figure 5. For both dyes, a marked negative effect of *IC* concentration on the biosorption capacity can be observed. It means that an increase of biomass concentration provokes a decrease of the biosorption capacity. Regarding pH, it does not show any effect on the biosorption capacity. It is important to highlight that the variable q was selected since the removal percentages remained practically constant (see Table 1). The dye removal percentages were around 75% for CV and 90% for MB. The optimal conditions for textile dye biosorption onto the biosorbent were obtained by determining the maximum point of surface responses (Figure 5). This way, the optimal process conditions for biosorption of CV were an *IC* concentration of 1 g L^{-1}, and as pH does not show any effect on the test response, pH 7 was selected for further experiments because at this pH value it was not necessary to use additional reagents to adjust the pH of medium. Under these conditions, the biosorption capacity was 36.5 mg g^{-1}. The optimal process conditions for biosorption of MB onto *IC* biomass were also 1 g L^{-1} *IC* concentration and pH 7, reaching a biosorption capacity of 45 mg g^{-1}.

Kinetic models evaluation

Figure 6 shows the biosorption kinetic curves of CV and MB on *IC* biomass at initial dye concentrations of 50 and 100 mg L^{-1}. A marked increase of biosorption capacity during the first minute can be observed, and after that, the increase of biosorption capacity was less than the previous one. The equilibrium was attained at around 90 min. Additionally, Figure 6 shows a higher biosorption capacity for MB than for CV dye, which could be related to steric effects from CV due to its size and distribution.

In order to obtain a suitable model that represents the kinetic results obtained experimentally, pseudo-first order and pseudo-second order models were fitted to experimental data. The selection of the more adequate model was based on the evaluation of R^2 and *ARE*. The kinetic parameters are given in Table 2. The high R^2 and the low *ARE* values show that the pseudo-second order model was the more suitable

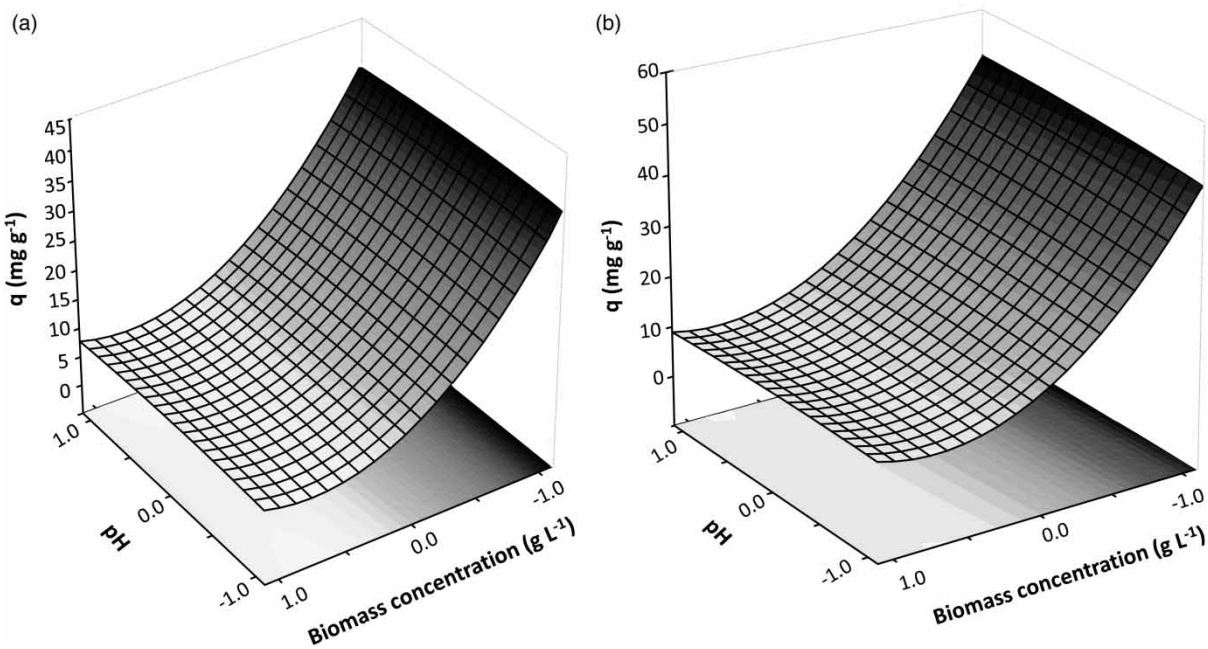

Figure 5 | Response surfaces of cationic dye biosorption capacity of *IC*: (a) CV and (b) MB.

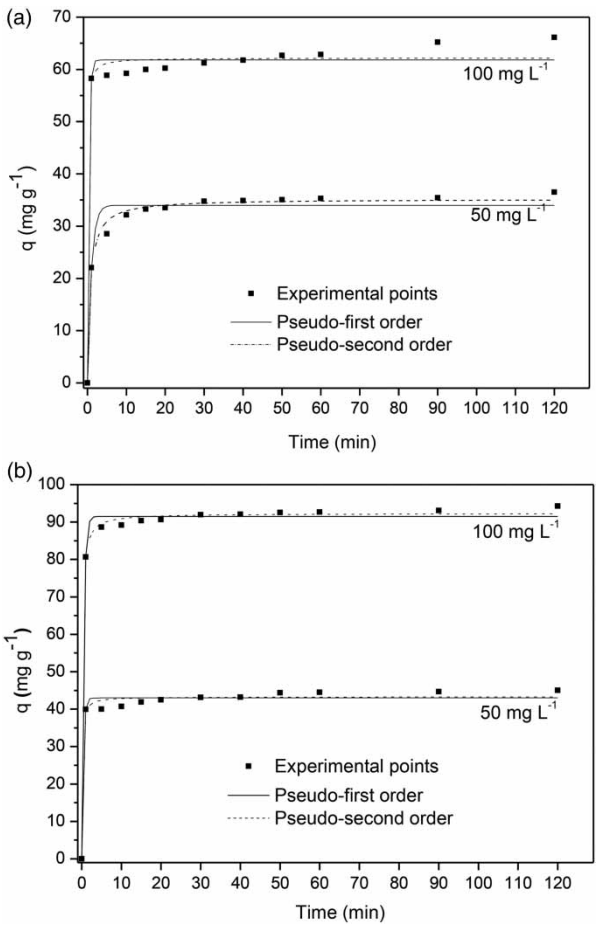

Figure 6 | Kinetic biosorption curves of (a) CV and (b) MB in the optimal conditions.

Table 2 | Kinetic parameters for CV and MB biosorption by *IC* biomass

	CV		MB	
Model	**50 mg L^{-1}**	**100 mg L^{-1}**	**50 mg L^{-1}**	**100 mg L^{-1}**
Pseudo-first order				
k_1 (min^{-1})	1.007	2.860	2.635	2.133
q_1 (mg g^{-1})	34.0	61.8	43.0	91.5
R^2	0.962	0.985	0.984	0.998
ARE (%)	4.34	2.82	2.95	1.46
Pseudo-second order				
k_2 (g mg^{-1} min^{-1})	0.041	0.188	0.209	0.071
q_2 (mg g^{-1})	35.2	62.2	43.3	92.3
h_0 (mg g^{-1} min^{-1})	50.8	727.3	391.8	604.9
R^2	0.990	0.987	0.988	0.998
ARE (%)	2.36	2.52	2.52	0.872
q_{exp} (mg g^{-1})	36.5	66.1	45.0	94.2

to represent the biosorption kinetic of CV and MB onto *IC* marine algae. The q_2 parameter shows higher values for MB than for CV, which is in accordance with observations derived from Figure 6. Moreover, the q_2 values increase from 50 to 100 mg L^{-1} for both dyes, confirming that the biosorption capacity is higher at higher concentrations. The h_0 (initial biosorption rate) values also increased with the initial MB and CV concentration, indicating that at the initial stages, the biosorption was faster when an initial concentration of 100 mg L^{-1} was used. On the other hand, it is important to mention the q_2 values are very close to the experimental data (q_{exp}), which confirms the predictive potentiality of the pseudo-second order model.

Equilibrium and thermodynamic results

Figure 7 exhibits the equilibrium isotherms of CV (Figure 7(a)) and MB (Figure 7(b)) dyes onto *IC* biomass under

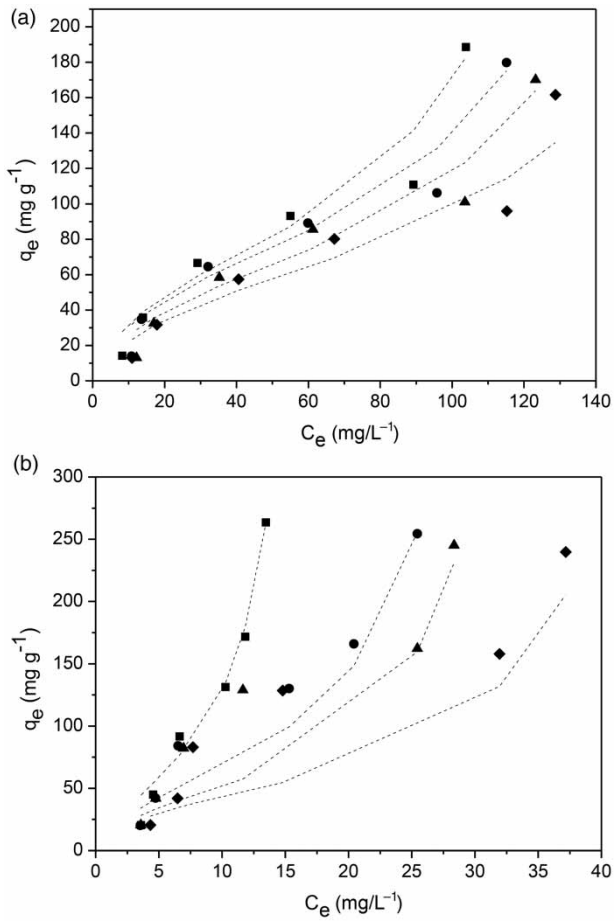

Figure 7 | Experimental biosorption equilibrium curves and BET isotherm model of CV (a) and MB (b) onto *IC* biosorbent. Temperatures: 298 K (■), 308 K (●), 318 K (▲), and 328 K (◆).

four different temperatures (298, 308, 318, and 328 K). According to Ruthven, it can be deduced that the isotherm curves obtained for both dyes were type II (Ruthven 1984). Figure 7 shows that the temperature increase provokes a decrease of dye biosorption capacity. This aspect makes the overall biosorption process more economical and clean, as it can be carried out at room temperature. The BET isotherm model was evaluated to fit the equilibrium data of CV and MB dyes onto the algal biosorbent. This model postulates that the initial adsorbed layer may act as a substrate for further biosorption stages; hence, the isotherm will be able to increase indefinitely (Mahmoud *et al.* 2012). The isotherm parameters are shown in Table 3. Considering the high values of R^2 and the low values of *ARE* obtained by the proposed model, it can be assumed that this model fit well the experimental data. The values of K_1 and K_2 decreased with the increase of temperature, which means that the biosorption process was favored at room temperature. Moreover, the increase of temperature caused a decrease of q_{BET} values from 65.9 to 56.1 and from 62.8 to 43.6 for CV and MB, respectively.

The thermodynamic parameters for the cationic dye biosorption onto *IC* algae are shown in Table 4. The R^2 values of the linear fit were 0.9367 and 0.9692 for CV and MB, respectively. In both cases, the negative values of ΔG^0 indicate that the biosorption processes were favorable and spontaneous at all the temperatures assayed. The negative values of enthalpy changes (ΔH^0) evidenced that the biosorption processes were exothermic. Furthermore, the magnitude of ΔH^0 suggested that physical interactions were involved in the biosorption processes (Piccin *et al.* 2011). The positive ΔS^0 values suggested the possibility of some structural changes or readjustments in the dye–macroalgae complex. This thermodynamic behavior has been also obtained by other authors (Dotto *et al.* 2013; Tabaraki & Heidarizadi 2016).

Comparison with adsorbents reported in the literature for CV and MB biosorption

It is important to mention that there are no biosorption studies reported in the literature for CV and MB onto *IC* red algae. A comparative study of some biosorption parameters allows us to show the strengths of the *IC* biosorbent with respect to other ones used and reported previously (Table 5). The studied biosorbent shows a biosorption capacity that is similar to or even better than that reported for other biosorbents used for biosorption of the same cationic dyes. Although two studies showed higher biosorption capacities than that of the present work, both

Table 3 | Isotherm parameters for CV and MB biosorption by *IC* biomass

	CV				MB			
Isotherm	**298 K**	**308 K**	**318 K**	**328 K**	**298 K**	**308 K**	**318 K**	**328 K**
BET								
K_1 (L mg^{-1})	0.0767	0.0745	0.0637	0.0565	0.287	0.252	0.320	0.284
K_2 (L mg^{-1})	0.0063	0.0056	0.0053	0.0047	0.0575	0.0303	0.0285	0.0213
q_{BET} (mg g^{-1})	65.9	64.8	59.4	56.1	62.8	60.7	45.3	43.6
R^2	0.9901	0.9943	0.9811	0.9963	0.9910	0.9893	0.9956	0.9938
ARE (%)	7.55	5.32	8.62	2.53	7.88	7.81	9.45	10.67

Table 4 | Thermodynamic parameters for CV and MB biosorption by *IC* biomass

	CV dye			MB dye		
T (K)	**ΔG^0 (kJ mol^{-1})**	**ΔH^0 (kJ mol^{-1})**	**ΔS^0 (kJ mol^{-1} K^{-1})**	**ΔG^0 (kJ mol^{-1})**	**ΔH^0 (kJ mol^{-1})**	**ΔS^0 (kJ mol^{-1} K^{-1})**
298	−21.11	−13.58	0.03	−24.25	−9.89	0.05
308	−21.69			−24.64		
318	−21.74			−25.29		
328	−21.93			−25.64		

Table 5 | Comparison of different adsorbents for the biosorption of CV and MB dyes

Biosorbent	Biosorption capacity (mg g^{-1})	pH	[Biosorbent] (g L^{-1})	Reference
Carica papaya seed	85.9[a]	8.0	12.0	Pavan *et al.* (2014)
Laminaria japonica alga	14.5[a]	10.0	5.0	Wang *et al.* (2008)
Eggshells	70.0[a]	8.0	30.0	Chowdhury *et al.* (2013)
Hevea brasillensis	18.8[a]	[c]	10.0	Tan & Hameed (2012)
Punica granatum husk	44.0[b]	5.0	12.0	Bretanha *et al.* (2016)
Gracilaria corticata alga	28.9[b]	8.0	5.0	Vijayaraghavan *et al.* (2016)
Solanum tuberosum peel	14.83[b]	6.0	0.7	Guechi & Hamdaoui (2016)
Olive stone	3.29[b]	7.0	5.0	Trujillo *et al.* (2016)
IC alga	36.5[a] 45.0[b]	7.0	1.0	This work

[a]For CV biosorption.
[b]For MB biosorption.
[c]Non reported.

employed high concentrations of biosorbent for the biosorption of CV at concentrations similar to those used in this contribution (Chowdhury *et al.* 2013; Pavan *et al.* 2014). This work exhibits an outstanding advantage of the *IC* biosorbent in comparison with the others presented in Table 5, which is related to the low biosorbent concentration needed for biosorption of the cationic dyes, turning the complete process into a more economical alternative, because the consumption of reagents is considerably reduced.

CONCLUSION

For the first time, this work demonstrates the potential of *IC* for cationic hazardous dye removal from aqueous solutions, following the concept of 'green chemistry', minimizing the use of additional reagents and the generation of toxic residues to the environment. FTIR spectra suggested that no links were formed during the biosorption processes. SEM images showed changes in the texture of the biosorbent surface, indicating an accumulation of the cationic dyes on that surface. Three-level two-factor 3^2 full factorial design showed that the optimum conditions for CV and MB biosorption were pH 7 and 1 g L^{-1} algae concentration. Under these conditions, the biosorption capacities were 36.5 and 45.0 mg g^{-1} for CV and MB dyes, respectively. The dye removal percentages were around 75% for CV and 90% for MB. Kinetic and equilibrium studies were performed. The pseudo-second order was the most suitable to describe the experimental data of the biosorption processes ($R^2 > 0.98$ and $ARE < 2.6$). The BET isotherm model represented adequately the biosorption of CV and MB onto the marine biosorbent. Based on the thermodynamic parameters, the biosorption processes were demonstrated to be exothermic, favorable and spontaneous at all the temperatures assayed. To sum up, an efficient, cheap, and environmentally friendly biosorption process has been proposed and studied for removal of hazardous cationic dyes from aqueous solutions.

ACKNOWLEDGEMENTS

The authors would like to thank National Council for Scientific and Technological Development (CNPq), Consejo Nacional de Investigaciones Científicas y Técnicas (CONICET), Agencia Nacional de Promoción Científica y Tecnológica (FONCYT) (Project PICT-2015-1338), and Universidad Nacional de Cuyo for the financial support.

REFERENCES

Ahmed, M. J. 2016 Application of agricultural based activated carbons by microwave and conventional activations for basic dye adsorption: review. *Journal of Environmental Chemical Engineering* **4** (1), 89–99.

Anantha Singh, T. S. & Ramesh, S. T. 2013 New trends in electrocoagulation for the removal of dyes from wastewater: a review. *Environmental Engineering Science* **30** (7), 333–349.

Anastopoulos, I. & Kyzas, G. Z. 2015 Progress in batch biosorption of heavy metals onto algae. *Journal of Molecular Liquids* **209**, 77–86.

Anastopoulos, I. & Kyzas, G. Z. 2016 Are the thermodynamic parameters correctly estimated in liquid-phase adsorption phenomena? *Journal of Molecular Liquids* **218**, 174–185.

Bretanha, M. S., Rochefort, M. C., Dotto, G. L., Lima, E. C., Dias, S. L. P. & Pavan, F. A. 2016 *Punica granatum* husk (PGH), a powdered biowaste material for the adsorption of methylene blue dye from aqueous solution. *Desalination and Water Treatment* **57** (7), 3194–3204.

Brunauer, S., Emmett, P. & Teller, E. 1938 Adsorption of gases in multimolecular layers. *Journal of the American Chemical Society* **60**, 309–319.

Castro, L., Bonilla, L. A., González, F., Ballester, A., Blázquez, M. L. & Muñoz, J. A. 2017 Continuous metal biosorption applied to industrial effluents: a comparative study using an agricultural by-product and a marine alga. *Environmental Earth Sciences* **76** (14), 491–498.

Chen, H., Zhao, J. & Dai, G. 2011 A new non-conventional and low-cost adsorbent for removal of methylene blue from aqueous solutions. *Journal of Hazardous Materials* **186** (2–3), 1320–1327.

Cheng, S., Oatley, D., Williams, P. & Wright, C. 2011 Characterisation and application of a novel positively charged nanofiltration membrane for the treatment of textile industry wastewaters. *Water Research* **46** (1), 33–42.

Chowdhury, S., Chakraborty, S. & Saha, P. D. 2013 Removal of crystal violet from aqueous solution by adsorption onto eggshells: equilibrium, kinetics, thermodynamics and artificial neural network modeling. *Waste and Biomass Valorization* **4** (3), 655–664.

Coates, J. 2000 Interpretation of infrared spectra, a practical approach. In: *Encyclopedia of Analytical Chemistry* (R. A. Meyers, ed.). Wiley, Chichester, UK, pp. 10815–10837.

Crini, G. & Badot, P. M. 2008 Application of chitosan, a natural aminopolysaccharide, for dye removal from aqueous solutions by adsorption processes using batch studies: a review of recent literature. *Progress in Polymer Science* **33** (4), 399–447.

Dadwal, A. & Mishra, V. 2017 Review on biosorption of arsenic from contaminated water. *Clean – Soil, Air, Water* **45** (7), article no. 1600364.

Devi, S. & Murugappan, A. 2016 Adsorption of basic magenta using fresh water algae and brown marine seaweed: characterization studies and error analysis. *Journal of Engineering Science and Technology* **11** (10), 1421–1436.

Dotto, G. L., Gonçalves, J. O., Cadaval, T. R. S. & Pinto, L. A. A. 2013 Biosorption of phenol onto bionanoparticles from *Spirulina* sp. LEB 18. *Journal of Colloid and Interface Science* **407**, 450–456.

Duygu, D., Udoh, A., Ozer, T., Akbulut, A., Erkaya, I., Yildiz, K. & Guler, D. 2012 Fourier transform infrared (FTIR) spectroscopy for identification of *Chlorella vulgaris* Beijerinck 1890 and *Scenedesmus obliquus* (Turpin) Kützing 1833. *African Journal of Biotechnology* **11** (16), 3817–3824.

Escudero, L. B., Maniero, M., Agostini, E. & Smichowski, P. N. 2016 Biological substrates: green alternatives in trace elemental preconcentration and speciation analysis. *TrAC – Trends in Analytical Chemistry* **80**, 531–546.

Esmaeili, A. & Darvish, M. 2014 Evaluation of the marine alga *Sargassum glaucescens* for the adsorption of Zn(II) from aqueous solutions. *Water Quality Research Journal of Canada* **49** (4), 339–345.

Guechi, E. K. & Hamdaoui, O. 2016 Biosorption of methylene blue from aqueous solution by potato (*Solanum tuberosum*) peel: equilibrium modelling, kinetic, and thermodynamic studies. *Desalination and Water Treatment* **57** (22), 10270–10285.

Ho, Y. & McKay, G. 1998 Kinetic models for the sorption of dye from aqueous solution by wood. *Process Safety and Environmental Protection* **76**, 183–191.

Jana, S., Purkait, M. K. & Mohanty, K. 2010 Removal of crystal violet by advanced oxidation and microfiltration. *Applied Clay Sciences* **50** (3), 337–341.

Kannan, S. 2014 FT-IR and EDS analysis of the seaweeds *Sargassum wightii* (brown algae) and *Gracilaria corticata* (red algae). *International Journal of Current Microbiology and Applied Sciences* **3** (4), 341–351.

Lagergren, S. 1898 About the theory of so-called adsorption of soluble substances. *Kongliga Svenska Vetenskapsakademiens Handlingar* **24**, 1–39.

Liang, H., Cao, X., Zhang, W.-J. & Yu, S. 2011 Robust and highly efficient free-standing carbonaceous nanofiber membranes for water purification. *Advanced Functional Materials* **21** (20), 3851–3858.

Mahmoud, M. E., Abdel-Fattah, T. M., Osman, M. M. & Ahmed, S. B. 2012 Chemically and biologically modified activated carbon sorbents for the removal of lead ions from aqueous media. *Journal of Environmental Science and Health, Part A* **47** (1), 130–141.

Mbacké, M. K., Kane, C., Diallo, N. O., Diop, C. M., Chauvet, F., Comtat, M. & Tzedakis, T. 2016 Electrocoagulation process applied on pollutants treatment-experimental optimization and fundamental investigation of the crystal violet dye removal. *Journal of Environmental Chemical Engineering* **4** (4), 4001–4011.

Milonjic, S. 2007 A consideration of the correct calculation of thermodynamic parameters of adsorption. *Journal of the Serbian Chemical Society* **72**, 1363–1367.

Mittal, A., Mittal, J., Malviya, A., Kaur, D. & Gupta, V. K. 2010 Adsorption of hazardous dye crystal violet from wastewater by waste materials. *Journal of Colloid and Interface Science* **343** (2), 463–473.

Moreno-Castilla, C. & Rivera-Utrilla, J. 2001 Carbon materials as adsorbents for the removal of pollutants from the aqueous phase. *MRS Bulletin* **26** (11), 890–894.

Navarro, N. P., Palacios, M., Mansilla, A. & Jofre, J. 2010 Morphological and growth alterations on early development stages of *Iridaea cordata* (Rhodophyta) under different intensities of UVB radiation. *Revista de Biologia Marina y Oceanografia* **45** (2), 255–265.

Pavan, F. A., Camacho, E. S., Lima, E. C., Dotto, G. L., Branco, V. T. A. & Dias, S. L. P. 2014 Formosa papaya seed powder

(FPSP): preparation, characterization and application as an alternative adsorbent for the removal of crystal violet from aqueous phase. *Journal of Environmental Chemical Engineering* **2** (1), 230–238.

Piccin, J. S., Dotto, G. L. & Pinto, L. A. 2011 Adsorption isotherms and thermochemical data of FD&C Red n° 40 binding by chitosan. *Brazilian Journal of Chemical Engineering* **28** (2), 295–304.

Rafatullah, M., Sulaiman, O., Hashim, R. & Ahmad, A. 2010 Adsorption of methylene blue on low-cost adsorbents: a review. *Journal of Hazardous Materials* **177** (1–3), 70–80.

Rautenberger, R., Huovinen, P. & Gómez, I. 2015 Effects of increased seawater temperature on UV tolerance of Antarctic marine macroalgae. *Marine Biology* **162** (5), 1087–1097.

Rivera-Utrilla, J., Bautista-Toledo, I., Ferro-Garca, M. A. & Moreno-Castilla, C. 2001 Activated carbon surface modifications by adsorption of bacteria and their effect on aqueous lead adsorption. *Journal of Chemical Technology and Biotechnology* **76** (12), 1209–1215.

Rubín, E., Rodríguez, P., Herrero, R. & Sastre De Vicente, M. E. 2010 Adsorption of methylene blue on chemically modified algal biomass: equilibrium, dynamic, and surface data. *Journal of Chemical & Engineering Data* **55** (12), 5707–5714.

Ruthven, D., 1984 *Principles of Adsorption and Adsorption Process*. Wiley, New York.

Sharma, P., Kaur, H., Sharma, M. & Sahore, V. 2011 A review on applicability of naturally available adsorbents for the removal of hazardous dyes from aqueous waste. *Environmental Monitoring and Assessment* **183** (1), 151–195.

Silverstein, R. M., Webster, F. X. & Kiemle, D. J. 2007 *Spectrometric Identification of Organic Compounds*. Wiley, New York, USA.

Song, J., Zou, W., Bian, Y., Su, F. & Han, R. 2011 Adsorption characteristics of methylene blue by peanut husk in batch and column modes. *Desalination* **265**, 119–125.

Suresh, B. & Ravishankar, G. A. 2004 Phytoremediation – a novel and promising approach for environmental clean-up. *Critical Reviews in Biotechnology* **24** (2–3), 97–124.

Tabaraki, R. & Heidarizadi, E. 2016 Simultaneous multidye biosorption by chemically modified *Sargassum glaucescens*: Doehlert optimization and kinetic, equilibrium, and thermodynamic study in ternary system. *Separation Science and Technology* **52** (4), 583–595.

Tan, I. A. W. & Hameed, B. H. 2012 Removal of crystal violet dye from aqueous solutions using rubber (*Hevea brasillensis*) seed shell-based biosorbent. *Desalination and Water Treatment* **48** (1–3), 174–181.

Trujillo, M. C., Martín-Lara, M. A., Albadarin, A. B., Mangwandi, C. & Calero, M. 2016 Simultaneous biosorption of methylene blue and trivalent chromium onto olive stone. *Desalination and Water Treatment* **57** (37), 17400–17410.

Umpierres, C., Prola, L., Adebayo, M., Lima, E., Dos Reis, G., Kunzler, D., Dotto, G., Arenas, L. & Bencenutti, E. 2017 Mesoporous Nb_2O_5/SiO_2 material obtained by sol-gel method and applied as adsorbent of crystal violet dye. *Environmental Technology* **38** (5), 566–578.

Ünnü, B., Gündüz, G. & Dükkancı, M. 2016 Heterogeneous Fenton-like oxidation of crystal violet using an iron loaded ZSM-5 zeolite. *Desalination and Water Treatment* **57** (25), 11835–11849.

Vijayaraghavan, J., Bhagavathi pushpa, T., Sardhar Basha, S., Vijayaraghavan, K. & Jegan, J. 2015 Evaluation of red marine alga *Kappaphycus alvarezii* as biosorbent for methylene blue: isotherm, kinetic and mechanism studies. *Separation Science and Technology* **50** (8), 1120–1126.

Vijayaraghavan, J., Bhagavathi Pushpa, T., Sardhar Basha, S. J. & Jegan, J. 2016 Isotherm, kinetics and mechanistic studies of methylene blue biosorption onto red seaweed *Gracilaria corticata*. *Desalination and Water Treatment* **57** (29), 13540–13548.

Wang, X. S., Liu, X., Wen, L., Zhou, Y., Jiang, Y. & Li, Z. 2008 Comparison of basic dye crystal violet removal from aqueous solution by low-cost biosorbents. *Separation Science and Technology* **43** (14), 3712–3731.

Weykam, G., Thomas, D. N. & Wiencke, C. 1997 Growth and photosynthesis of the Antarctic red algae *Palmaria decipiens* (Palmariales) and *Iridaea cordata* (Gigartinales) during and following extended periods of darkness. *Phycologia* **36** (5), 395–405.

Yahiaoui, I., Aissani-Benissad, F., Madi, K., Benmehdi, N., Fourcade, F. & Amrane, A. 2013 Electrochemical pre-treatment combined with biological treatment for the degradation of methylene blue dye: Pb/PbO_2 electrode and modeling-optimization through central composite design. *Industrial & Engineering Chemistry Research* **52** (42), 14743–14751.

Yang, C., Li, L., Shi, J., Long, C. & Li, A. 2015 Advanced treatment of textile dyeing secondary effluent using magnetic anion exchange resin and its effect on organic fouling in subsequent RO membrane. *Journal of Hazardous Materials* **284**, 50–57.

Yao, Y., Zhao, C., Zhao, M. & Wang, X. 2013 Electrocatalytic degradation of methylene blue on PbO_2-ZrO_2 nanocomposite electrodes prepared by pulse electrodeposition. *Journal of Hazardous Materials* **263**, 726–734.

Zhang, H., Wu, J., Wang, Z. & Zhang, D. 2010 Electrochemical oxidation of crystal violet in the presence of hydrogen peroxide. *Journal of Chemical Technology and Biotechnology* **85** (11), 1436–1444.

First received 3 May 2017; accepted in revised form 12 September 2017. Available online 25 September 2017